Electronic transport in the metallic state of oriented poly(*p*-phenylenevinylene)

M. Ahlskog, Reghu M., and A. J. Heeger
Institute for Polymers and Organic Solids, University of California at Santa Barbara, Santa Barbara, California 93106

T. Noguchi and T. Ohnishi
Sumitomo Chemical Co. Ltd., Tsukuba Research Laboratory, Tsukuba, Ibaraki, 300-32, Japan
(Received 16 January 1996; revised manuscript received 28 February 1996)

The room-temperature electrical conductivity of tensile-drawn and oriented poly(*p*-phenylenevinylene), PPV, doped with sulfuric acid (H_2SO_4) is approximately 10^4 S/cm for current along the draw direction; the anisotropy $\sigma_\parallel/\sigma_\perp \approx 100$ where $\sigma_\parallel$ and $\sigma_\perp$ refer to the conductivity parallel to and perpendicular to the axis of orientation. The resistivity, $\rho(T)$, is nearly temperature independent with a weak negative temperature coefficient, $\rho_r \equiv \rho(1.3\ \mathrm{K})/\rho(200\ \mathrm{K}) \approx 1.07-1.3$. A positive temperature coefficient (resistivity) appears below 20 K. The magnetoconductance (MC) is anisotropic and dependent on the direction of the applied magnetic field with respect to the chain axis. When the field is perpendicular to the chain axis, the MC is positive and nearly independent of temperature at low fields; at high fields, the MC gradually decreases as the temperature is lowered from 4.2 to 1.3 K. When the field is parallel to the chain axis, the MC is negative. The MC is nearly identical, however, when the current direction is parallel and perpendicular to the chain axis. The temperature dependence of the conductivity and the rich interplay of positive and negative MC arises from the importance of weak localization (WL) and electron-electron (e-e) interactions. Specifically, the anisotropy of the MC is shown to result from the anisotropy of the WL contribution. The contributions from WL and e-e interactions were verified from $[\Delta\sigma(H,T)/T^{1/2}]$ vs (H/T) plots. [S0163-1829(96)03822-2]

I. INTRODUCTION

During the last few years, metallic properties have been observed in a wide range of novel materials.[1] Among these the ''metallic'' state has been consistently observed in various high-quality conducting polymers. These doped conjugated polymers are disordered metals; the temperature dependences of conductivity, thermopower, susceptibility and magnetoconductance in doped polyacetylene $(CH)_x$, polypyrrole (PPy), and polyaniline (PANI) are characteristic of disordered metals near the boundary of the metal-insulator transition.[2] The quasi-one-dimensional (1D) nature of such linear chain systems, the competing roles of interchain interactions and disorder, the interplay of band and diffusive charge transport, the importance of localization and correlation effects, and the anisotropic transport parameters in oriented systems have provided an opportunity to observe unique features in the metallic state in conducting polymers. Among the various transport properties, magnetoconductance (MC) is a particularly sensitive probe of the transport mechanism in disordered metallic systems. MC measurements in oriented metallic polyacetylene $[(CH)_x]$ have shown the importance of weak localization (WL) and electron-electron (e-e) interactions to the low-temperature transport.[3] It is of considerable importance to confirm these results in other metallic conducting polymers.

Ohnishi *et al.*[4] reported that the room-temperature conductivity, σ(300 K), of tensile-drawn and oriented PPV doped with H_2SO_4 is of the order of 10^4 S/cm. Previously Madsen *et al.*[5] reported metallic conduction in arsenic pentafluoride (AsF_5)-doped, oriented PPV samples, with a room-temperature conductivity of 2400 S/cm. However, more extensive measurements of the transport properties are lacking. We have carried out measurements of the temperature dependence and magnetic-field dependence of the anisotropic conductivity in oriented samples of PPV-H_2SO_4; the results are reported here. Detailed analysis of $\sigma(T)$ in directions parallel and perpendicular to chain axis indicates that the localization-interaction model is consistent with the data in both cases, although the conductivities $[\sigma_\parallel$ vs $\sigma_\perp]$ differ by two orders of magnitude. This is similar to the results obtained from oriented metallic polyacetylene[3(a)] and polypyrrole.[6] Thus the bulk transport properties of oriented metallic conducting polymers imply that these systems are anisotropic three-dimensional (3D) conductors. This is in agreement with theoretical arguments which indicate that interchain interactions[7] and polymer chain-dopant interactions[8] are substantial in conducting polymers. In this sense, conducting polymers appear to be rather different from other quasi-one-dimensional systems (e.g., the charge-transfer salts). We find that the e-e interaction contribution to the low-temperature conductivity is important in metallic samples. In particular, the good fit to $\sigma(T) \propto T^{1/2}$ below 4.2 K (at 0 and 8 T) is consistent with the interaction contribution. A positive temperature coefficient of the resistivity (TCR) has been observed in some samples, as in PPy doped with phosphorous pentafluoride (PF_6).[6] We present here a detailed study of the MC in oriented metallic PPV-H_2SO_4. In general, the MC is positive at low fields and negative at higher fields when the field is perpendicular, while it is exclusively negative when field is parallel to the chain axis. The positive and negative MC are attributed to WL and e-e interaction contributions, respectively.[9] A similar anisotropic MC has been observed in oriented metallic iodine-doped polyacetylene $[\text{I-}(CH)_x]$.[3(a)]

TABLE I. The values of $\sigma(200\ \mathrm{K})$, $\sigma_0[\sigma(T=0\ \mathrm{K})]$, ρ_r, m, and m_H [Eqs. (2) and (3)] for metallic PPV-H_2SO_4 samples and the parameters obtained from the data analysis using the localization-interaction model for magnetoconductance (MC). To the right are the ratios of the field of maximums of MC, $H_{\max}$, with the corresponding temperature. In the lower section are the configurations of the current and field directions with respect to chain axis for the different samples.

Sample	$\sigma(200\ \mathrm{K})$[a]	σ_0[a]	ρ_r[d]	m[b]	m_H[b]	B_{EE^a}[c]	B_{EE}[c]	$H_{\max}/T$ 1.3 K	$H_{\max}/T$ 2.5 K
$M_1^{\parallel}$	15 200	12 530	1.21	54	180	−130	−112	1.6	1.6
$M_2^{\parallel}$	9 540	9 050	1.07	−100	−48	−53	−46	≅2	≅2
$M_1^{\perp}$	120	91.6	1.30	0.56	2.53	−1.53	−1.83	0.8	0.8
$M_2^{\perp}$	109	96.0	1.13	0.01	1.09	−0.97	−0.96	≅2	≅2
$M_3^{\parallel}$	6 860	5 420	1.25	42	140	−81	−85		

$M_1^{\parallel}$, $M_2^{\parallel}$: **H**⊥chain∥**j**
$M_1^{\perp}$: **H**⊥chain, **j**⊥chain, **H**⊥**j**
$M_2^{\perp}$: **H**⊥chain, **j**⊥chain, **H**∥**j**
$M_3^{\parallel}$: **H**∥chain∥**j**

[a]In S/cm.
[b]In S/cm $K^{1/2}$.
[c]In S/cm $T^{1/2}$.
[d]$\rho_r=\rho(1.3\ \mathrm{K})/\rho(200\ \mathrm{K})$.

II. EXPERIMENTAL PROCEDURES

Free standing films of PPV were prepared from a precursor polymer containing cyclic sulfide as described by Ohnishi *et al.*[4] Film thicknesses were in the range from 3 to 5 μm. All measurements are carried out on tensile-drawn samples with draw ratio 10:1. Because the spin concentration in carefully prepared PPV is only about 1 spin per 10^6 PPV monomer units, sp^3 defects are unimportant in these samples.[10] Measurements of the dichroic ratio at 1520 cm^{-1} gives values for the optical anisotropy of 40–50 indicating that the PPV chains are highly oriented after tensile drawing. The typical length and width of samples prepared for conductivity measurements are 8 and 1 mm, respectively.

The samples were immersed in 96% H_2SO_4 for approximately 1 h for doping. The conductivity of each sample was optimized by *in situ* conductivity measurements as a function of doping time. When the conductivity reached the maximum, the samples were cooled immediately to prevent degradation. Since the presence of any residual sulfuric acid in the sample could induce small variations in conductivity at temperatures above 200 K the data are shown only below 200 K at which all the chemistry associated with the doping process and all ionic motion are frozen.

For measurement of $\sigma_{\parallel}$ and $\sigma_{\perp}$, the samples were cut with the long axis parallel and perpendicular to the draw axis (chain axis). Conductivity measurements used the standard four-probe method with platinum pressure contacts; the contact resistance was typically less than 10 Ω. The MC measurements were carried out by the standard four-probe method by using platinum pressure contacts; typically, the contact resistance was less than 10 Ω. The measurements were carried out in a superconducting magnet cryostat (8–10 T) with the samples immersed in liquid helium for measurements below 4.2 K.[3(a)] The directions of field and the current with respect to the chain axis for various samples are shown in Table I. Temperature was measured with a calibrated Cernox™ sensor. The power dissipated in the sample was less than 1 μW at low temperatures. The temperature dependence $\sigma(T)$ was reproducible during thermal cycling.

III. RESULTS AND DISCUSSION

A. Temperature dependence of conductivity

The temperature dependences of the conductivities of two samples ($M_1^{\parallel}$ and $M_2^{\parallel}$) cut with the long axis parallel to the chain axis and one sample ($M_2^{\perp}$) cut with the long axis perpendicular are shown in Fig. 1. The resistivity ratios, $\rho_r\approx\rho(1.3\ \mathrm{K})/\rho(200\ \mathrm{K})$, of the three samples are shown in Table I; the ρ_r values are even lower than obtained from the best polyacetylene samples. Thus, based on the transport properties, PPV-H_2SO_4 can be considered the ''most metallic'' conducting polymer.

The values of ρ_r are rather similar for transport parallel and perpendicular to the chain axis. Thus, an anisotropic 3D model is appropriate for describing the transport properties. Although $\sigma_{\parallel}$ is much higher than the typical value of Mott's minimum metallic conductivity in systems near the metal-insulator transition, $\sigma_{\perp}$ is rather close to the Mott value. This implies that interchain transport is the limiting factor for observing metallic transport in these systems.

Slight differences in $\sigma(T)$ at low temperatures are seen in different samples as shown for $\sigma_{\parallel}(T)$ in Fig. 2. Similar variations from sample to sample are observed in $\sigma_{\perp}(T)$. The sample-to-sample variation is common in doped conducting polymers where these differences arise from slight variations in the doping level and/or the degree of disorder.[2] In heavily doped inorganic semiconductors a similar variation of the sign of the TCR is observed close to the metal-insulator boundary, and can also be quantitatively related to the doping concentration.[11]

The presence of large finite conductivity for both $\sigma_{\parallel}(T)$ and $\sigma_{\perp}(T)$ as $T\rightarrow 0$ and the positive TCR for $M_2^{\parallel}$ (below 20

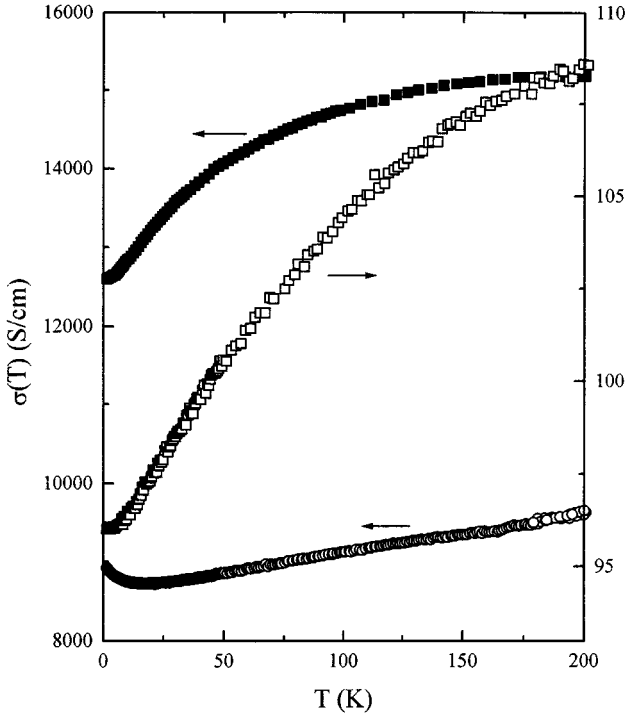

FIG. 1. Conductivity vs temperature for metallic PPV-H_2SO_4 samples: (■) for $M_1^{\parallel}$, (□) for $M_2^{\perp}$, and (○) for $M_2^{\parallel}$.

K) suggests that the usual expression for $\sigma(T)$ for disordered metallic systems can be used for PPV-H_2SO_4, although one must take into account the anisotropy in microscopic transport parameters (diffusion coefficient, etc.). The conductivity of disordered metallic systems is given by[9,11]

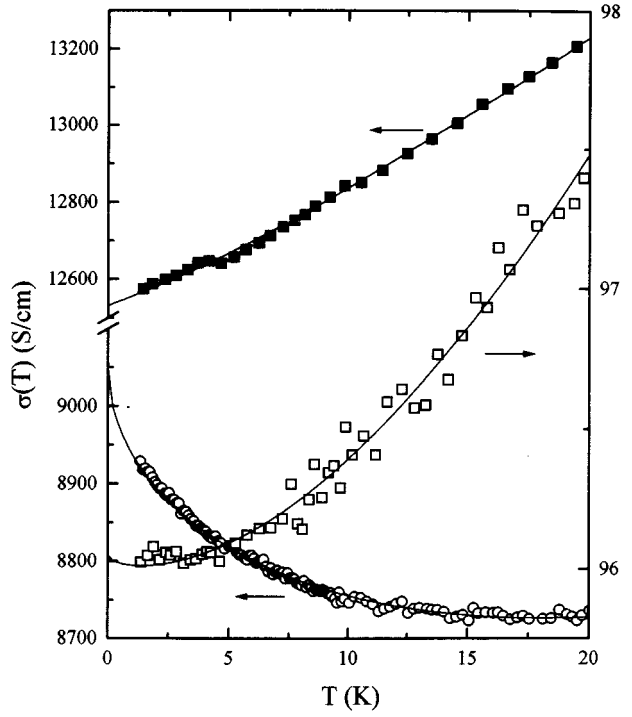

FIG. 2. Conductivity vs temperature ($T<20$ K) for metallic PPV-H_2SO_4 samples: (■) for $M_1^{\parallel}$, (○) for $M_2^{\parallel}$, and (□) for $M_2^{\perp}$: The fit to Eq. (1) $[\sigma(T)=\sigma_0+mT^{1/2}+BT^{p/2}]$ is shown by the solid line and the fitting parameters are shown in Table II.

TABLE II. The values of fitting parameters in Eq. (1). $[\sigma(T)=\sigma_0+mT^{1/2}+BT^{p/2}]$ for metallic PPV-H_2SO_4 samples ($M_1^{\parallel}$, $M_2^{\parallel}$, and $M_2^{\perp}$).

Sample	m	B	p
$M_1^{\parallel}$	18.5	14.8	2.5
$M_2^{\parallel}$	−116	2.1	3
$M_2^{\perp}$	−0.04	0.009	3.5

$$\sigma(T)=\sigma_0+mT^{1/2}+BT^{p/2} \tag{1}$$

with

$$m=\alpha[(4/3)-(3\gamma F_{\sigma}/2)]. \tag{2}$$

The second term ($T^{1/2}$) results from e-e interactions, and the third term is the correction to σ_0 due to localization effects. The value of p is determined by the temperature dependence of the scattering rate $[\tau^{-1}\propto T^p]$ from the dominant dephasing mechanism. For electron-phonon scattering, $p=3$; for inelastic e-e scattering, $p=2$ in the clean limit or $p=3/2$ in the dirty limit. The Hartree factor (F) is the screened interaction averaged over the Fermi surface; $\alpha=(e^2/\hbar)(1.3/4\pi^2)(k_B/2\hbar D)^{1/2}$ is a parameter depending on the diffusion coefficient (D), and γF_{σ} is the interaction parameter ($\gamma F_{\sigma}>0$). The value of γ depends on the band structure.[9,11] The prefactor m in the interaction term depends on the magnetic field. When the field exceeds the limit for Zeeman splitting ($g\mu_B H>k_B T$, where g is the g value of the electron and μ_B is the Bohr magneton) the value of m changes to

$$m_H=\alpha[(4/3)-(\gamma F_{\sigma}/2)]. \tag{3}$$

Although the interplay of weak localization and e-e interaction contributions is sensitive to the extent of disorder present in the system, generally the former is dominant at higher temperatures and lower fields and the latter is dominant at lower temperatures and higher fields, as we will show in the next section with the MC measurements.

In order to check the validity of this model, Eq. (1) was fitted to the data for all samples; the fitting parameters are given in Table II. The fits were done by first determining the zero-temperature conductivity σ_0 from $T^{1/2}$ plots of the conductivity below 4 K, assuming the last term in Eq. (1) can be omitted in the zero-temperature limit since usually $p>1$. The m (and m_H) values thus obtained are shown in Table I. Then the p values were fixed and m and B allowed to vary freely. This was repeated for several p values until the best fits were found. The best-fit curves fall quite well on the data points ($T<20$ K) as shown in Fig. 2. The agreement spans a sufficiently wide temperature range that the weak localization and interaction contributions are both important. The fits yield $p\approx 3\pm 0.5$, implying that electron-phonon scattering ($p=3$) is the dominant dephasing mechanism. The sign of m is negative for sample $M_2^{\parallel}$ ($m<0$ is the origin of the positive TCR), implying that $\gamma F_{\sigma}>8/9$, and positive for sample $M_1^{\parallel}$. The magnitude of γF_{σ} (and therefore the sign of m) is known to be sensitive to the degree of disorder.[8] As shown in Table I, $M_2^{\parallel}$ has a smaller resistivity ratio, implying that this sample is slightly more ''metallic.'' Among the perpendicu-

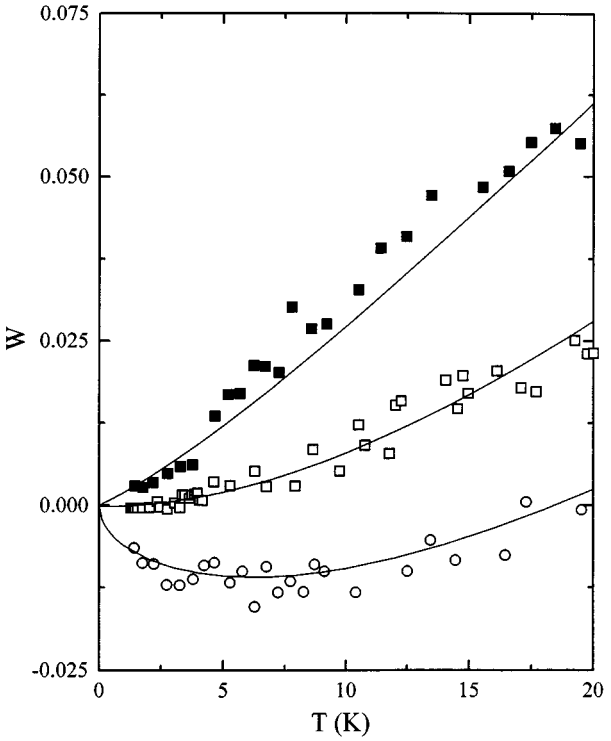

FIG. 3. w (where, $w(T)=[0.5mT^{1/2}+(p/2)BT^{p/2}]/\sigma(T)$) vs T for metallic PPV-H_2SO_4 samples: (■) for $M_1^{\parallel}$, (○) for $M_2^{\parallel}$, and (□) for $M_2^{\perp}$.

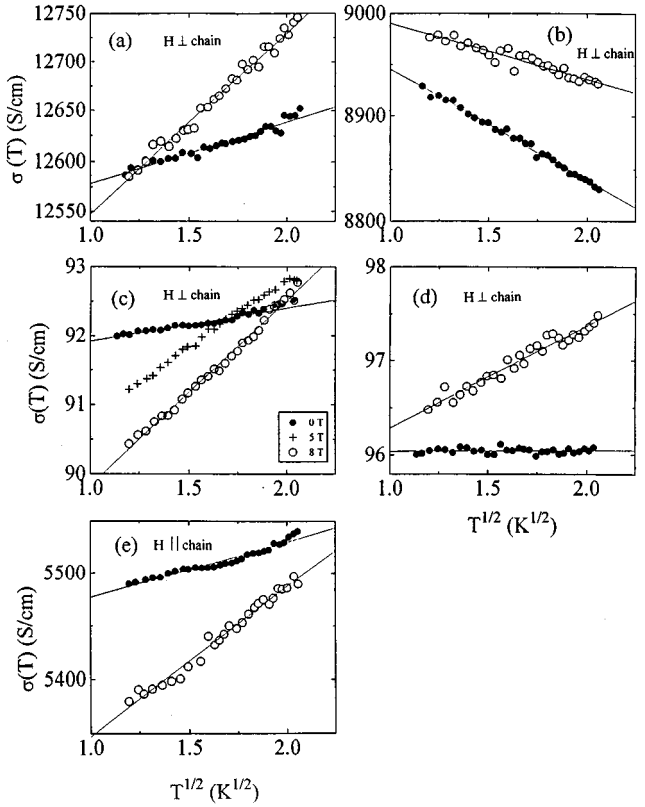

FIG. 4. Conductivity vs $T^{1/2}$ for metallic PPV-H_2SO_4 samples at zero field (●) and 8 T (○) fields [5 T also in (c)]: (a) $M_1^{\parallel}$, (b) $M_2^{\parallel}$, (c) $M_1^{\perp}$, (d) $M_2^{\perp}$, and (e) $M_3^{\parallel}$. The direction of the field (**H**) with respect to the chain direction are indicated in the figures. The full configuration (**H**, current, chain) is shown in Table I.

lar cut samples m is very small for $M_2^{\perp}$ and negative for $M_1^{\perp}$, again showing the variation in low-temperature conduction properties that follow from subtle differences in the doping conditions. The m values obtained from the fitting (Table II) and those obtained if the weak localization term $BT^{p/2}$ is omitted (Table I) are not in precise agreement. Indeed, the fitting suffers from the lack of data obtained below 1 K. However, even when such data are available, e.g., for other materials, the determination of the parameters m and B from $\sigma(T)$ alone is somewhat crude. For accurate insight into WL and e-e interaction effects magnetoconductance measurements are necessary.

The validity of the model was verified by the following suggestion of Möbius[12] who noted that in the disordered metallic regime, the logarithmic derivative, $w(T)=d\ \ln\sigma/d\ \ln T$, is far more sensitive than $\sigma(T)$ itself as expressed by Eq. (1). The logarithmic derivative of Eq. (1) is given by

$$w(T)=[0.5mT^{1/2}+(p/2)BT^{p/2}]/\sigma(T). \tag{4}$$

Equation (4) implies that $w(T)$ vanishes as $T\rightarrow 0$ for metallic samples. Using the parameters obtained from Fig. 2 (see Table II), Eq. (4) provides an excellent fit to the data, as shown in Fig. 3. The excellent agreement shown in Figs. 2 and 3 implies that the localization-interaction model developed for disordered metals on the metallic side of the metal-insulator transition provides a good description of the transport in metallic PPV.

Although this analysis of $\sigma(T)$ shows that the localization-interaction model is appropriate, other models for charge transport might also satisfactorily explain the same data. It is well known that the localization-interaction contributions to conductivity are quite sensitive to magnetic field. Therefore, we have tested the validity of the localization-interaction model by measuring the field dependence of conductivity.

The temperature dependences of conductivities of all the samples below 4.2 K and at zero field and 8 T are shown in Fig. 4 as a function of $T^{1/2}$. We also measured the temperature dependence at 5 T; for visual clarity the 5 T data are shown only in Fig. 4(c), as a representative example. Both parallel (a,b,e; $M_1^{\parallel}$, $M_2^{\parallel}$, and $M_3^{\parallel}$, respectively) and perpendicular (c,d; $M_1^{\perp}$,$M_2^{\perp}$) cut samples are shown. In all cases the TCR becomes more negative, independent of the direction of the field with respect to the chain and current directions. Furthermore, within this temperature regime the data are consistent with $T^{1/2}$ behavior, implying that the e-e interaction term [$mT^{1/2}$, Eq. (2)] dominates the temperature dependence in this temperature regime. In Figs. 4(a)–4(d), the MC is positive at higher temperatures, implying WL effects. However, as we will show below, the temperature dependence is still dominated by e-e interaction since the WL magnetoconductance is rather temperature independent.[13] Thus, within the e-e interaction picture, the temperature dependence is easily explained by the Zeeman splitting which causes the change of the prefactor m [Eq. (2)] to m_H [Eq. (3)]. Since γF_{σ} is always positive, $m_H>m$, in agreement

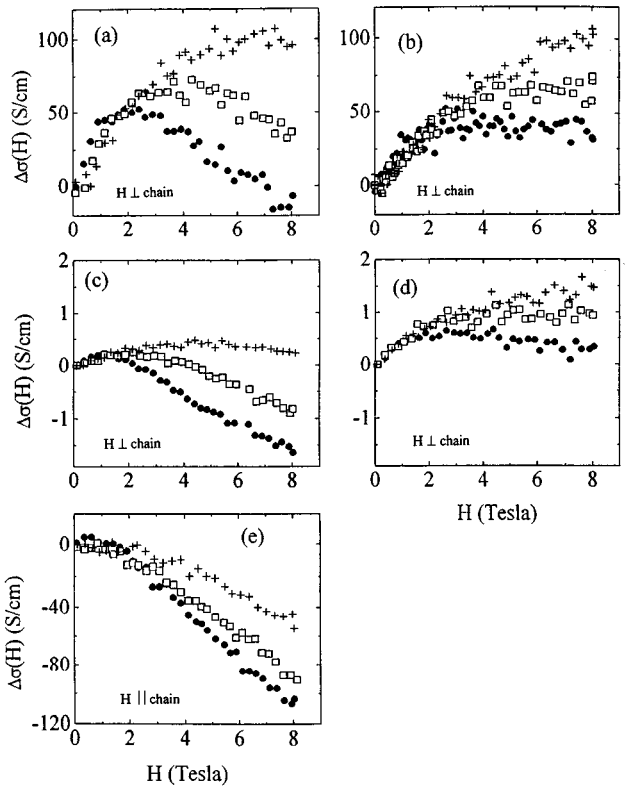

FIG. 5. Magnetoconductance vs field at 4.2 K (+), 2.5 K (□), 1.3 K (●) for the same samples as in Fig. 4.

with the observed behavior. The prefactor changes to m_H when the Zeeman splitting is greater than k_BT, i.e., $H/T \gg 0.7$ T/K. At 8 T and below 4.2 K this condition is quite well satisfied, while at 5 T the limit is approached close to 4.2 K. Indeed, slight bending of the 5 T temperature dependence data towards the slope of the zero-field data may be discerned, as shown in Fig. 4(c).

B. Magnetoconductance

In Fig. 5 we show the MC data obtained with the field either perpendicular (a–d, transverse MC) or parallel (e, longitudinal MC) to the chain axis. In the transverse MC the direction of the current j varies as shown in Table I. At low fields the positive MC dominates the transverse case while at higher fields the MC turns to negative. At low fields, the positive MC is nearly temperature independent. As noted in Sec. III A, the principal difference between samples $M_1^{\parallel}$ [5(a)] and $M_2^{\parallel}$ [5(b)] is that the TCR below 4.2 K is negative for $M_1^{\parallel}$ and positive for $M_2^{\parallel}$. Nevertheless, the general behavior of the MC is essentially identical and characteristic of the field perpendicular configuration.

We emphasize again that the behavior of the transverse MC when the current is perpendicular to the chain axis (samples $M_1^{\perp}, M_2^{\perp}$) is rather similar to the case when the current is parallel to the chain axis ($M_1^{\parallel}, M_2^{\parallel}$), although $\sigma_{\parallel}/\sigma_{\perp} \approx 10^2$ and $\sigma_{\perp}(300\ \mathrm{K}) \approx 10^2$ S/cm (near the Mott minimum metallic conductivity). The positive MC in sample $M_1^{\perp}$ is weaker than in other samples. This lower value is probably related to its slightly higher resistivity ratio (Table I) which shows it to be closer to the metal-insulator transition, where the positive MC vanishes.[14] Thus, both the temperature dependence of conductivity and the behavior of the MC are similar whether the current is parallel or perpendicular to chain axis, indicating that the transport mechanism is similar in directions parallel and perpendicular to chain axis. High-quality oriented metallic conducting polymers behave like anisotropic 3D metals.

A dramatically different behavior is observed when both field and current are parallel to chain axis (sample $M_3^{\parallel}$) as shown in Fig. 5(e). In this case, the MC is negative at all temperatures and field strengths; the positive MC is apparently absent. This anisotropic behavior of the MC (when the field is parallel or perpendicular to chain axis direction) is fully consistent with that observed in oriented metallic I-$(CH)_x$.[3(a)]

Following the discussion on the temperature dependence, we analyze the MC as an interplay between the WL and e-e interaction effects. The former yields positive MC (in the absence of spin-orbit effects) while the latter gives negative MC. Both effects are apparent in the case of transverse MC, in samples $M_1^{\parallel}, M_2^{\parallel}, M_1^{\perp}, M_2^{\perp}$, [Figs. 5(a)–5(d)], while the longitudinal MC of sample $M_3^{\parallel}$ [Fig. 5(e)] displays different behavior. We will therefore analyze the two cases separately.

The WL and e-e interaction contributions to the MC are considered as additive. Thus, the total low-field MC ($g\mu_B H \ll k_B T$, for e-e interaction) is given by the following expression:[3(a),9,11]

$$\Delta\Sigma_L(H,T) = (1/12\pi^2)(e/c\hbar)^2 G_0 (l_{\mathrm{in}})^3 H^2 - 0.041(g\mu_B/k_B)^2 \alpha\gamma F_\sigma T^{-3/2} H^2, \quad (5)$$

where the first and second terms on the right-hand side result from WL and e-e interactions, respectively; $G_0 = (e^2/\hbar)$, and l_{in} is the inelastic scattering length.

At high fields, the positive (negative) MC due to WL (e-e interaction) is proportional to $H^{1/2}$. Thus, the total high-field MC is given as[3(a),9,11]

$$\Delta\Sigma_H(H) = B_{\mathrm{WL}} H^{1/2} + B_{\mathrm{EE}} H^{1/2}, \quad (6a)$$

where

$$B_{\mathrm{EE}} = -0.77(g\mu_B/k_B)^{1/2} \alpha\gamma F_\sigma \quad (g\mu_B H \gg k_B T). \quad (6b)$$

The first term on the right-hand side of Eq. (6a) describes the contribution form WL (B_{WL} is a numerical constant at high magnetic fields), and the second term the contribution from the e-e interaction.

The characteristic behavior of the transverse MC provides an indication of the crossover fields (low- to high-field regimes, positive to negative MC). All the (transverse) MC data at 1.3 or 2.5 K exhibit a maximum in positive MC at H_{max}, although this is broadened considerably when the positive component is strong. This maximum depends on the temperature. The ratio of H_{max}/T at both 1.3 and 2.5 K are shown in Table I; H_{max}/T is roughly constant for each transverse MC sample, and quite accurately so for samples $M_1^{\parallel}$ and $M_1^{\perp}$ where H_{max} can be unambiguously determined. For the e-e interaction contribution, the high-field limit [Eq. (6b)] is valid when the Zeeman splitting is greater than k_BT; i.e., $H/T \gg 0.7$ T/K. The constant value of H_{max}/T for each

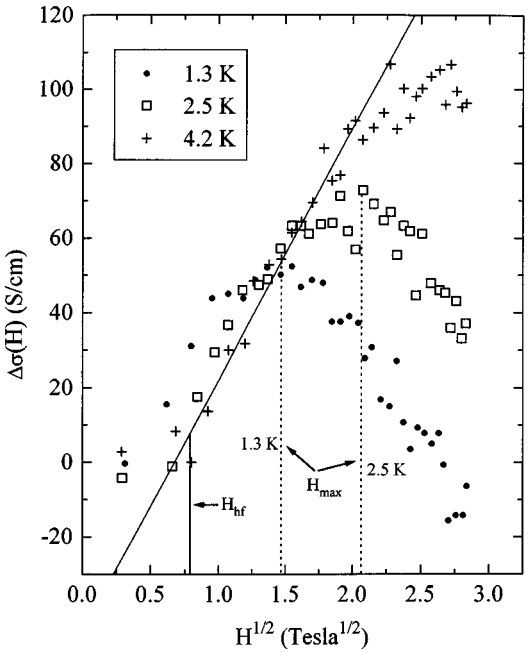

FIG. 6. Magnetoconductance of sample $M_1^{\parallel}$ in a $H^{1/2}$ scale. The vertical solid line shows the lower limit, $H_{\rm hf}$, to $H^{1/2}$ dependence. The dotted lines show the fields $H_{\rm max}$ at maximum positive magnetoconductance at 1.3 and 2.5 K.

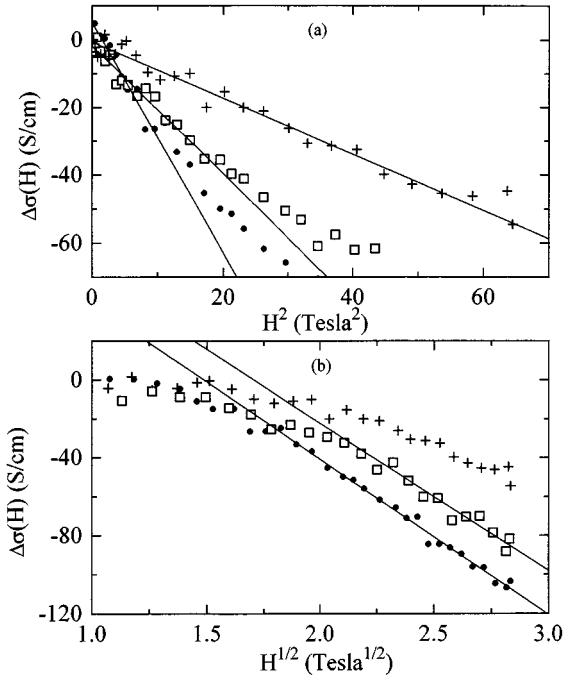

FIG. 7. Magnetoconductance vs field for current and field parallel to chain axis; sample $M_3^{\parallel}$, (a) H^2 dependence at low field; (b) $H^{1/2}$ dependence at high field.

sample, together with the fact that in all cases $H_{\rm max}/T>0.7$ T/K indicates that the peaks in the MC data [Figs. 5(a)–5(d)] follow from the onset of high-field behavior for the *e-e* interaction contribution [Eq. (5b)]. Figure 6 shows the MC of sample $M_1^{\parallel}$ in a $H^{1/2}$ scale, illustrating the high-field limits of both *e-e* interaction and WL. The $H_{\rm max}$ values are indicated for the 1.3 and 2.5 K data. At 4.2 K the $H_{\rm max}/T$ ratio would suggest $H_{\rm max}$ to be at 7–8 T for this sample. Indeed, the MC at 4.2 K clearly levels off at these fields. Generally, however, our measurements were not performed at high enough fields to get the $H_{\rm max}/T$ ratio at 4.2 K. The slopes of the negative MC at higher fields (1.3, 2.5 K) are nearly parallel at different temperatures as shown in Figs. 5 and 7(b), in agreement with *e-e* interaction theory.

At fields below $H_{\rm max}$ the data roughly overlap at different temperatures, as in Fig. 6, indicating that the positive MC contribution is nearly temperature independent at low fields. For the WL contribution, the high-field limit[9] [Eq. (5)] is defined by $H>\Phi_0/l_{\rm in}^2$, where Φ_0 is the flux quantum ($\hbar/2e$). From the data in Fig. 6, one can estimate the lower limit of the field ($H_{\rm hf}$, indicated with solid vertical line) at which the positive MC due to WL follows the $H^{1/2}$ dependence; $H_{\rm hf}\approx 0.6\pm 0.2$ T. Thus, since $H_{\rm hf}\leqslant\Phi_0/l_{\rm in}^2$, this gives as the lower limit for $l_{\rm in}$ 240 Å, in reasonable agreement with the value estimated for polyacetylene.[3(a)]

The importance of the *e-e* interaction contribution was shown in the previous section by the $T^{1/2}$ dependence of conductivity, at zero field and at 8 T, where the prefactors of the $T^{1/2}$ term were m and m_H, respectively. These data can be related to the observed MC as follows. Since $\alpha\gamma F_\sigma=(m_H-m)$, Eqs. (2) and (3), the values of $B_{\rm EE}$ [Eq. (6b)] can be obtained from the temperature dependence of conductivity at 0 and 8 T (see Table I). These values of $B_{\rm EE}$ were cross checked from those obtained from the MC data at 1.3 and 4.2 K ($B_{\rm EE*}$), which have a $H^{1/2}$ dependence at high fields [Eq. (6b)]. Since the weak localization contribution $B_{\rm WL}$ is temperature independent, it is cancelled out by subtracting the values of $\Delta\Sigma_H(H)$ at 4.2 K from those at 1.3 K. Therefore, the resulting values $[B_{\rm EE*}=\Delta\Sigma_H(H,T=1.3\ {\rm K})-\Delta\Sigma_H(H,T=4.2\ {\rm K})]$, result only from the *e-e* interaction contribution. The consistency of the values of $B_{\rm EE}$ (from $T^{1/2}$ dependence of $\sigma(T)$] and $B_{\rm EE*}$ (from $H^{1/2}$ dependence of $\Delta\Sigma_H(H)$] is shown in Table I. The most serious disagreement comes from sample $M_1^{\perp}$, which has a weak positive MC and thus is difficult to analyze accurately. If the WL contribution at high field [$H^{1/2}$ dependence in Eq. (6)] is not taken into account, then the values of $B_{\rm EE}$ and $B_{\rm EE*}$ are in gross disagreement for all samples. This analysis quite satisfactorily explains the behavior of the transverse MC in any of the configurations used for samples $M_1^{\parallel}$, $M_2^{\parallel}$, $M_1^{\perp}$, and $M_2^{\perp}$. The values of various parameters obtained from the analysis are summarized in Table I.

Since only negative MC can be discerned in the longitudinal MC of sample $M_3^{\parallel}$, the dominant contribution to the MC results from the *e-e* interaction. The H^2 dependence of the low-field MC for $M_3^{\parallel}$ is shown in Fig. 7(a). The slope of the H^2 dependence increases, and the upper limit of the field for the H^2 dependence is reduced when the temperature is lowered from 4.2 to 1.3 K, consistent with the temperature dependence of the *e-e* interaction contribution which results from Zeeman splitting.[9,11] The values of the slopes are -3 4, -1.9, and -0.85 S/cm T^2 at 1.4, 2.5, and 4.2 K, respectively, in reasonable agreement with those obtained (-4.44, -1.86, and -0.85 S/cm T^2 at 1.4, 2.5, and 4.2 K) from the temperature dependence data, calculated from m and m_H. Thus, the principal contribution to the negative MC at low field for $M_3^{\parallel}$ results from the *e-e* interaction.

At higher fields the MC follows the $H^{1/2}$ dependence [Eq.

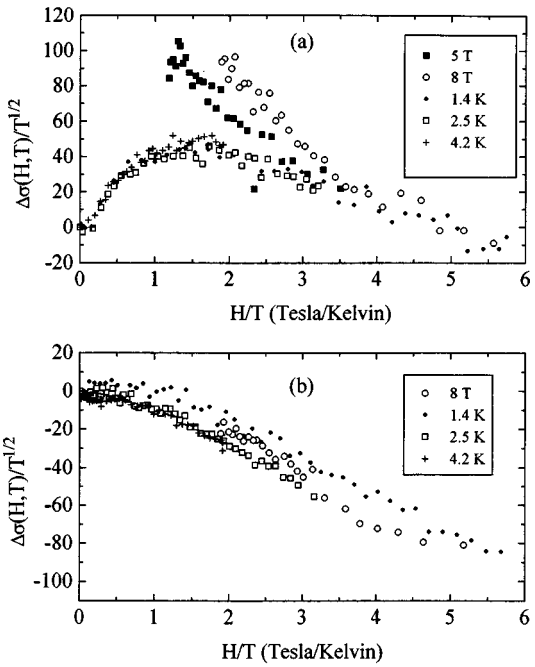

FIG. 8. The $[\Delta\sigma(H,T)/T^{1/2}]$ vs (H/T) plots: (a) For current (field) parallel (perpendicular) to chain axis, sample $M_1^{\parallel}$; (b) For current and field parallel to chain axis, sample $M_3^{\parallel}$. The data come from the temperature dependence (1.3–4.2 K) at 5 and 8 T and from magnetoconductance (0–8) at 1.3, 2.5, and 4.2 K.

6(b)], as shown in Fig. 7(b). Since the slopes of $H^{1/2}$ dependence are nearly temperature independent; these data directly yield the values of $B_{\mathrm{EE}*}$. This value was again cross checked with that obtained (B_{EE}) by substituting the values of $\alpha\gamma F_{\sigma}$ (from the temperature dependence of conductivity at 0 and 8 T) in Eq. (6). The values of B_{EE} and $B_{\mathrm{EE}*}$ are in excellent agreement as shown in Table I. *From the analysis above we may conclude that the WL contribution is negligible when the field is parallel to chain axis*. Thus the consistency of the data analysis for all samples is in accord with the localization-interaction model.

C. Electron-electron interaction contribution: Scaling of magnetoconductance

Recently, Bogdanovich *et al.*[15] reported a universal scaling behavior in the MC that results from the *e-e* interaction contribution and presented an elegant method to distinguish the contributions from WL and *e-e* interactions. They have observed that the *e-e* interaction contribution to MC follows an universal scaling behavior given by

$$\Delta\sigma(H,T)=\sigma(H,T)-\sigma(0,T)\propto T^{1/2}f(H/T), \qquad (7)$$

where $f(H/T)$ is consistent with that predicted by the interaction theory [see Eq. (3.44b) in Ref. 9]. Equation (7) follows the general formula for conductivity in a magnetic field. The $[\Delta\sigma(H,T)/T^{1/2}]$ vs (H/T) plots for the conductivity data as a function of temperature and field for samples $M_1^{\parallel}$ and $M_3^{\parallel}$ are shown in Figs. 8(a) and 8(b), respectively. The difference in the behavior of $\Delta\sigma(H,T)$ when the field is perpendicular ($M_1^{\parallel}$, transverse MC) and parallel ($M_3^{\parallel}$, longitudinal MC) to the chain axis is obvious. The expected universal scaling behavior in MC due to the dominant contribution from *e-e* interaction is clearly shown in Fig. 8(b) up to 8 T in the temperature range 4.2–1.3 K in the case of longitudinal MC (sample $M_3^{\parallel}$). However, in the case of transverse MC (sample $M_1^{\parallel}$), the deviation from the scaling behavior is shown in Fig. 8(a), which indicates the importance of WL contribution when the field is perpendicular to chain axis. For the configuration of sample $M_3^{\parallel}$, all the data over the entire temperature and field range follow the expected universal behavior showing that the WL contribution is negligible; the *e-e* interaction contribution is dominant when the field is parallel to chain axis. This is again consistent with the observations in Fig. 5. The range of H/T values in Fig. 8 is small compared to that in Ref. 15 where millikelvin data is available. However, since in this material rich MC behavior appears in the temperature range where our measurements were done our use of this method should be justified.

D. Weak localization contribution: Anisotropic magnetoconductance

The accumulated data from various works on electronic transport in oriented conducting polymers indicates that the anisotropy of conductivity $\sigma_{\parallel}/\sigma_{\perp}$ is not a function of variables such as temperature or hydrostatic pressure. This suggests that the observed anisotropy, $\sigma_{\parallel}/\sigma_{\perp}\cong 100$ in our case, does not result simply from the microscopic structure, or intrinsic factors of the polymer. However, the anisotropic behavior of MC presented in this work should be a tool that probes transport at the microscopic level. The same subtle interplay of WL and *e-e* interaction contributions to the MC was also observed in iodine doped oriented polyacetylene films,[3(a)] where the directional dependence of the MC was also extensively investigated. From this and the present work we may conclude that the MC is determined by the orientation of the chain axis with respect to the field. A similar weak contribution to positive MC has been observed in other studies on oriented conducting polymers[3(b),16] and also in carbon fibers when the field is parallel to the fiber axis.[17] These, and other systems that may exhibit similar phenomena [e.g., SN_x (Ref. 18)] have in common the uniaxial symmetry.

We have argued in this work (Sec. III B) that the anisotropy is specifically due to the anisotropic behavior of weak localization. Previously the orbital character of the scattering that leads to WL has been utilized in two different systems to measure the effect on the MC. The underlying principle behind these experiments is that some dimension of the system is less than the inelastic scattering length l_{in}. By measuring MC along thin cylinders where the radius is less than l_{in} and thus the charge carriers confined to paths around the cylinder, the MC has been found to weakly oscillate as a function of the field parallel to the cylinder axis, with the flux quantum Φ_0 as the period (Ref. 9 and references therein). Moreover, in case of 2D metal films, with a thickness less than l_{in}, the positive MC is nearly absent when the field is parallel to the plane of the film and the MC is positive when the field is perpendicular to the plane of the film [Ref. 19 and refs. therein]. (In the presence of spin-orbit interaction the situation is more complicated.)

In a simplified picture the WL effect on MC is determined by the flux Φ enclosed by a typical backscattering path of the charge carrier (analogous to the Bohm-Aharonov effect). This flux is $\Phi \propto H^* l_{\rm in}^2$ in a normal isotropic medium. The directional effects imposed on the WL magnetoconductance described above were due to geometrical constraints to the backscattering paths that affect the flux in a way that depends on the direction of the field. In the case of anisotropic conductors with a uniaxial symmetry such as in our case we propose that the anisotropy of WL is due to very unequal fluxes Φ that a certain magnetic-field intensity produces when the field is parallel to the chain axis ($\Phi^{\parallel}$, longitudinal MC) and when it is perpendicular to it ($\Phi^{\perp}$, transverse MC). The unequality arises from the inelastic scattering length which in a anisotropic conductor with uniaxial symmetry may be considered the geometrical mean of a longitudinal scattering length $l_{\rm in}^{\parallel}$ (along the chain direction) and a transverse $l_{\rm in}^{\perp}$ (perpendicular to chain direction). The flux Φ is determined by the normal cross section of the charge carrier backscattering paths with respect to the field direction. In the longitudinal case the flux $\Phi^{\parallel}$ is then proportional to $l_{\rm in}^{\perp 2}$, while in the transverse case $\Phi^{\perp} \propto l_{\rm in}^{\perp} * l_{\rm in}^{\parallel}$. Numerical values for $l_{\rm in}$ is not available since the macroscopic transport is not entirely determined by it, as noted above. It is, however, clear that $l_{\rm in}^{\parallel} > l_{\rm in}^{\perp}$, and thus $\Phi^{\perp} > \Phi^{\parallel}$. This result then roughly explains the reduced WL contribution in the longitudinal MC as compared to the transverse case.

We noted above that the anisotropy of MC has been observed previously in other conducting polymers. However, except for iodine-doped, equally anisotropic, oriented polyacetylene films,[3(a)] no other polymer has to our knowledge exhibited as highly anisotropic MC as PPV-H_2SO_4, testifying to the quality and the high degree of orientation of this material.

IV. CONCLUSION

Doped oriented PPV can be considered as one of the best metallic conducting polymers with values of σ(300 K) and ρ_r which are similar to those of metallic $(CH)_x$. In fact, for the best PPV-H_2SO_4 samples, $\rho_r \sim 1.07$ is slightly lower than obtained in the best $(CH)_x$ samples ($\rho_r \sim 1.2$). In both cases, the low-temperature conductivity is consistent with the localization-interaction model but with different parameters (consistent with the high anisotropy); $d \ln \sigma / d \ln T$ vanishes as $T \rightarrow 0$ as expected for disordered metallic systems on the metallic side of the metal-insulator transition. The observation of a positive TCR (below 20 K), which decreases in magnitude in a magnetic field, confirms the importance of interaction contribution in the metallic regime. The enhancement of conductivity in a transverse magnetic field at temperatures above 2.5 K and the gradual suppression of this effect at lower temperatures shows the dominance of weak localization and *e-e* interaction contributions, respectively, at different temperatures. The behavior of MC in oriented metallic PPV-H_2SO_4 samples shows strongly anisotropic features. When the field is perpendicular to chain axis ($M_1^{\parallel}$), the positive MC resulting from weak localization is nearly temperature independent at low fields; a negative contribution from the *e-e* interaction appears at high fields. The crossover is related to the $H_{\rm max}/T$ ratio, due to the Zeeman splitting which accounts for the MC in the *e-e* interaction contribution. Although $\sigma_{\parallel}/\sigma_{\perp}$ is nearly 100, the behavior of MC is nearly identical for current parallel ($M_1^{\parallel}, M_2^{\parallel}$) and perpendicular ($M_1^{\perp}, M_2^{\perp}$) to the chain axis. When the field is parallel to chain axis ($M_3^{\parallel}$), the MC is negative at all temperatures (4.2–1.3 K) for $H \leqslant 8$ T. This negative MC exhibits H^2 and $H^{1/2}$ dependences at low and high fields, respectively. This implies that the *e-e* interaction contribution is dominant and that the WL contribution is negligible when the field is parallel to the chain axis. The universal scaling behavior of negative MC due to *e-e* interaction is observed when the field is parallel to chain axis ($M_3^{\parallel}$) from the $[\Delta\sigma(H,T)/T^{1/2}]$ vs (H/T) plots. When the field is perpendicular to chain axis ($M_1^{\parallel}$), the deviation from the universal scaling results from the importance of the WL contribution at low fields. Thus, the anisotropy in MC in oriented polymers with uniaxial symmetry provides another opportunity to separate the WL and *e-e* interaction effects. Furthermore, this anisotropy in MC is a valuable tool since it probes the anisotropy at the microscopic level which is masked by the morphological structure in the macroscopic conductivity.

ACKNOWLEDGMENTS

This research was supported by the Office of Naval Research (Kenneth Wynne, Program Officer). M. Ahlskog thanks the Neste Oy Foundation (Finland) for a personal grant.

[1] P. W. Anderson, Phys. World **8**, 37 (1995).

[2] Reghu Menon, C. O. Yoon, D. Moses, and A. J. Heeger, in *Handbook of Conducting Polymers*, 2nd ed., edited by T. A. Skotheim, R. L. Elsenbaumer, and J. R. Reynolds (Dekker, New York, 1996); R. S. Kohlman, J. Joo, and A. J. Epstein, in *Physical Properties of Polymers Handbook*, edited by J. Mark (AIP, New York, 1996); Reghu Menon, in *Conductive Organic Molecules and Polymers*, edited by H. S. Nalwa (Wiley, New York, 1996).

[3] (a) Reghu M., K. Väkiparta, Y. Cao, and D. Moses, Phys. Rev. B **49**, 16 162 (1994); (b) Y. Nogami, H. Kaneko, H. Ito, T. Ishiguro, T. Sasaki, N. Toyota, A. Takahashi, and J. Tsukamoto, *ibid.* **43**, 11 829 (1991).

[4] T. Ohnishi, T. Noguchi, T. Nakano, M. Hirooka, and I. Murase, Synth. Met. **41-43**, 309 (1991).

[5] J. M. Madsen, B. R. Johnson, X. L. Hua, R. B. Hallock, M. A. Masse, and F. E. Karasz, Phys. Rev. B **40**, 11 751 (1989).

[6] C. O. Yoon, Reghu M., D. Moses, and A. J. Heeger, Phys. Rev. B **49**, 10 851 (1994).

[7] S. Stafström, Synth. Met. **65**, 185 (1994); **69**, 667 (1995); Phys. Rev. B **51**, 4137 (1995); M. Springborg and L. A. Eriksson, Synth. Met. **57**, 4302 (1993); L.A. Eriksson and M. Springborg, Phys. Rev. B **46**, 15 833 (1992).

[8] R. J. Cohen and A. J. Glick, Phys. Rev. B **42**, 7659 (1990); A. Yamashiro, A. Ikawa, and H. Fukutome, Synth. Met. **65**, 233 (1994).

[9] P. A. Lee and T. V. Ramakrishnan, Rev. Mod. Phys. **57**, 287 (1985).
[10] S. Kuroda, T. Nogushi, and T. Ohnishi, Phys. Rev. Lett. **72**, 286 (1994).
[11] P. Dai, Y. Zhang, and M. P. Sarachick, Phys. Rev. B **45**, 3984 (1992).
[12] A. Möbius, Phys. Rev. B **40**, 4194 (1989).
[13] P. Lindqvist, J. Phys. Condens. Matter **4**, 177 (1992).
[14] M. Ahlskog, Reghu M., A. J. Heeger, T. Noguchi, and T. Ohnishi (unpublished)
[15] S. Bogdanovich, P. Dai, M. P. Sarachik, and V. Dobrosavljevic, Phys. Rev. Lett. **74**, 2543 (1995).
[16] H. H. S. Javadi, A. Chakraborty, C. Li, N. Theophilou, D. B. Swanson, A. G. MacDiarmid, and A. J. Epstein, Phys. Rev. B **43**, 2183 (1991).
[17] A. W. P. Fung, M. S. Dresselhaus, and M. Endo, Phys. Rev. B **48**, 14 953 (1993).
[18] K. Kaneto, K. Yoshino, and Y. Inuishi, in *Electronic Properties of Inorganic Quasi-One-Dimensional Compounds*, edited by P. Monceau (Kluwer, Dordrecht, 1985).
[19] G. Bergmann, Phys. Rep. **107**, 39 (1984).